Selected Paper

Structure and Electronic Properties of Biferrocene–TCNQ Charge-Transfer Complexes: Effects of Acceptors and Crystal Environment on the Mixed-Valence States

Tomoyuki Mochida,* Shizue Yamazaki, Shinya Suzuki, Setsuko Shimizu, and Hatsumi Mori†

Department of Chemistry, Faculty of Science, Toho University, Miyama, Funabashi, Chiba 274-8510

†Institute for Solid State Physics, The University of Tokyo, Kashiwanoha, Kashiwa, Chiba 277-8581

Received July 10, 2003; E-mail: mochida@chem.sci.toho-u.ac.jp

Correlations between the valence states, crystal structure, and electronic states in biferrocenium charge-transfer complexes with tetracyanoquinodimethane (TCNQ) acceptors have been revealed. Structural determination of (1′,1‴-dipropyl-1,1″-biferrocenium)$^+$(TCNQ)$_3^-$ (**1**) and (1′,1‴-dibutyl-1,1″-biferrocenium)$^+$(TCNQ)$_3^-$ (**2**) showed that these complexes form a 1:3 segregated stack structure, and are semiconductors. Stabilization of the averaged valence states in the biferrocenium cations in **1** and **2** is attributed to the symmetrical environment around the cations and to the shielding of the dipole–dipole interactions by the TCNQ columns. Structural determination of (biferrocenium)$^+$(F$_4$TCNQ)$^-$ (**3**) and (1′,1‴-diethyl-1,1″-biferrocenium)$^+$(F$_4$TCNQ)$^-$ (**4**) revealed that **3** has a segregated structure, while **4** exhibits a 2:2 mixed-stack structure, represented as …D$^+$D$^+$A$^-$A$^-$D$^+$D$^+$A$^-$A$^-$…. Valence localization in the biferrocenium cations in these complexes can be rationalized by electrostatic interactions between the cations and the anions in addition to the low crystal symmetry. All the complexes show paramagnetic susceptibilities, which mainly arise from the contribution of the donor molecules.

Electron transfer phenomena in mixed-valence molecular materials have attracted much attention because of their possible application in molecular devices.[1–5] Biferrocenium salts are typical mixed-valence compounds (Fig. 1), and extensive studies have been carried out for years on their electron transfer processes by means of ^{57}Fe Mössbauer spectroscopy.[1,6] More recently, intriguing phenomena, such as phase isomerization associated with valence change, have been discovered in some biferrocenium salts by Nakashima et al.[7–9] The valence states of biferrocenium salts can be divided into three groups: trapped-valence (Group Ⅰ), temperature-dependent valence (Group Ⅱ), and average-valence (Group Ⅲ). In Group Ⅱ, the electrons are localized at low temperatures, and valence averaging occurs with increasing temperature. Many biferrocenium salts with inorganic anions have been synthesized to date, and factors affecting their valence states have been investigated in detail: (i) the intermolecular cation–cation and anion–cation interactions, (ii) the packing effect, and (iii) the symmetry of the cation, or the zero-point energy difference.[7–13] However, there are fewer examples of biferrocenium organic charge-transfer complexes, and the factors affecting the valence states in these materials are less well understood. Intrigued by the ferromagnetic interactions in ferrocene–TCNQ-type complexes,[14] we aimed to design molecular magnets with accompanying dielectric functions by combining biferrocenium cations with organic acceptors.[15–17] Thus, we consider it important to obtain an insight into the mechanism of electron transfer and valence ordering phenomena in biferrocenium charge-transfer complexes.

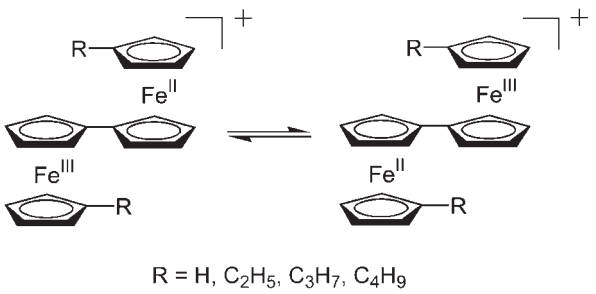

Fig. 1. Valence tautomerization of biferrocenium cations coupling with electron transfer.

Several biferrocenium TCNQ complexes have been synthesized to date. Among the known biferrocenium salts, the TCNQ complexes seem to be exceptional from the viewpoint of their valence states, because electron transfer processes in these salts survive at low temperatures (Group Ⅲ), while biferrocenium salts with inorganic anions often undergo valence ordering transitions at temperatures higher than ~200 K (Groups Ⅰ and Ⅱ).[9] Nakashima et al. has reported on the valence states in (1′,1‴-dipropyl-1,1″-biferrocenium)$^+$(TCNQ)$_3^-$ (**1**) and (1′,1‴-dibutyl-1,1″-biferrocenium)$^+$(TCNQ)$_3^-$ (**2**), which are valence detrapped at temperatures as low as 77 K.[18,19] The origin of the stable average valence states is highly interesting. Iijima et al. has reported on the preparation of charge-transfer salts with tetrafluorotetracyanoquinodimethane (= F$_4$TCNQ), (biferrocenium)$^+$(F$_4$TCNQ)$^-$ (**3**) and (1′,1‴-diethyl-1,1″-biferrocenium)$^+$(F$_4$TCNQ)$^-$ (**4**).[20] These compounds are valence trapped at room temperature. The contrasting valence behaviors of compounds **1**–**2** and **3**–**4**, depending on the acceptor species, attracted our attention. We considered it necessary to reveal the origin of these different valence states for the future development of functional materials based on mixed-valency.

Published on the web December 15, 2003; DOI 10.1246/bcsj.76.2321

In this paper, we report on the correlation between the structure and properties in these mixed-valent salts, and discuss the role of the acceptors in terms of the crystal structure and valence states. This work comprises the basic part of our investigation on biferrocene–TCNQ-type complexes; preparation of non-mixed-valent complexes and their electronic properties will be reported in a subsequent paper.[21]

Experimental

Materials and Methods. The charge-transfer salts of **1**–**4** were synthesized according to the literature methods,[18,20] and crystals suitable for X-ray crystallography were grown by slow evaporation of dichloromethane solutions. We could grow single crystals of four charge-transfer complexes out of eight combinations of the two acceptors and four donors, while others were powders. Magnetic susceptibilities were measured with a SQUID magnetometer in the temperature range 2–300 K under a magnetic field of 5000 G. The core diamagnetic components were corrected by calculation from Pascal's constants. Electrical conductivities for **1** and **2** were measured on single crystals along the needle axes, which were the stacking axis, by using the four-probe method. Gold paste and 15 μm gold wires were used for the electrical contact with the electrodes. Thermal analysis was performed on MAC Science DSC 3100 in the temperature range 90–330 K, at the heating rate of 5 K min^{-1}. Intermolecular overlap integrals were estimated based on extended Hückel molecular orbital calculations,[22] using a software package supplied by Prof. Takehiko Mori (Tokyo Institute of Technology).

X-ray Crystallography. The X-ray diffraction measurements were performed at 296 K on Rigaku AFC-5S and Rigaku AFC-7R four-circle diffractometers using graphite-monochromated Mo Kα radiation ($\lambda = 0.71069$ Å). Reflections within the range of $2\theta < 55^\circ$ were collected, of which reflections with $I > 2\sigma(I)$ were used for refinements. Crystal data, data collection parameters, and analysis statistics for **1**–**4** are listed in Table 1. The structures were solved by the direct method (SIR92)[23] and refined by using the teXsan[24] or CrystalStructure[25] software packages. The hydrogen atoms were placed at idealized positions and allowed to ride on the relevant heavier atoms. Empirical absorption corrections were applied (Ψ scan). Selected bond lengths (Å) and angles (°) for the cations in **1**–**4** are listed in Table 2. Selected bond lengths for the acceptors are listed in Table 3. Crystallographic data (excluding structure factors) for the structures in this paper have been deposited with the Cambridge Crystallographic Data Centre as supplementary publication nos. CCDC 204513 (**1**), 204514 (**2**), 204515 (**3**), and 204516 (**4**). Copies of the data can be obtained, free of charge, on application to CCDC, 12 Union Road, Cambridge CB2 1EZ, UK, (fax: +44-1223-336-033 or e-mail: deposit@ccdc.cam.ac.uk).

Results

Crystal Structures of the Averaged-Valence Complexes. Structural determination of compounds **1** and **2** revealed that both compounds exhibited segregated-stack structures. In these 1:3 D:A stoichiometry compounds, both the donor and acceptor molecules exhibit mixed-valency; the donor molecules exist as monocations,[18] and thus the formal charge on the acceptors is −0.33. The bond lengths of the acceptors (Table 3) are in-between the values for TCNQ and its monoanion,[26] although it is difficult to precisely estimate the degree of charge transfer from the bond lengths.

Figure 2(a) shows an ORTEP[27] drawing of the cations in compound **1**, together with the numbering scheme. Figure 3(a) shows the packing diagram of compound **1**, and a projection along the stacking direction ($a + c$) is depicted in Fig. 3(b). Figure 4 shows the packing diagram of compound **2**. In both complexes, the biferrocenium monocations sit on the inversion center, and the two ferrocene units are crystallographically equivalent. The alkyl substituents have the all-trans conforma-

Table 1. Crystallographic Data for **1**–**4**

	1	**2**	**3**	**4**
Empirical formula	$C_{62}H_{42}N_{12}Fe_2$	$C_{64}H_{46}N_{12}Fe_2$	$C_{32}H_{18}N_4F_4Fe_2$	$C_{36}H_{26}N_4F_4Fe_2$
Formula weight	1066.79	1094.84	646.21	702.32
Crystal dimensions/mm	0.5 × 0.2 × 0.2	0.5 × 0.2 × 0.1	0.2 × 0.1 × 0.1	0.6 × 0.3 × 0.1
Crystal system	triclinic	triclinic	monoclinic	triclinic
Space group	$P\bar{1}$ (No. 2)	$P\bar{1}$ (No. 2)	$P2_1/n$ (No. 14)	$P\bar{1}$ (No. 2)
a/Å	11.285(2)	11.389(4)	7.211(3)	12.509(2)
b/Å	14.601(4)	15.568(4)	15.62(5)	13.953(2)
c/Å	8.306(2)	8.336(3)	23.33(1)	9.043(1)
α/°	99.28(2)	105.12(3)		90.51(1)
β/°	111.26(2)	109.78(3)	96.59(4)	100.83(1)
γ/°	83.42(2)	74.81(2)		103.09(1)
V/Å^3	1256.4(5)	1318.0(8)	2609(2)	1507.7(4)
Z	1	1	4	2
d_{calcd}/g cm^{-3}	1.410	1.379	1.645	1.547
μ(Mo Kα)/cm^{-1}	6.33	6.05	11.70	10.20
Diffractometer	Rigaku AFC5S	Rigaku AFC5S	Rigaku AFC7R	Rigaku AFC5S
No. of reflection	6054	6463	6736	7246
No. of observation	3394	4334	3547	4156
Refl./Parameter ratio	9.4	12.3	12.8	10.3
R_1[a]; R_w[b]	0.065; 0.154	0.091; 0.223	0.043; 0.130	0.049; 0.128
Goodness of fit	1.01	1.06	1.54	1.25

a) $R_1 = \Sigma||F_o| - |F_c||/\Sigma|F_o|$. b) $R_w = [\Sigma w(F_o^2 - F_c^2)^2/\Sigma w(F_o^2)^2]^{1/2}$.

Table 2. Selected Bond Lengths (Å) and Angles (°) for Biferrocenium Cations in **1**–**4**

1			
Distances		C(4)–C(4)[e]	1.449(9)
Fe(1)–C(Cp1[a])	2.068(6)–2.097(5)	Fe(1)–C(Cp2[b])	2.051(6)–2.114(6)
(Avg.)	2.079	(Avg.)	2.075
C–C(Cp1[a])	1.409(9)–1.427(8)	C–C(Cp2[b])	1.376(9)–1.430(9)
(Avg.)	1.417	(Avg.)	1.406
Fe(1)–Cp1[a]	1.694(3)	Fe(1)–Cp2[b]	1.695(3)
Angle		Cp1[a]–Cp2[b]	4.9(3)
2			
Distances		C(4)–C(4)[e]	1.447(9)
Fe(1)–C(Cp1[a])	2.055(4)–2.092(4)	Fe(1)–C(Cp2[b])	2.053(5)–2.099(6)
(Avg.)	2.067	(Avg.)	2.064
C–C(Cp1[a])	1.409(8)–1.435(6)	C–C(Cp2[b])	1.37(1)–1.45(1)
(Avg.)	1.421	(Avg.)	1.406
Fe(1)–Cp1[f]	1.677(3)	Fe(1)–Cp2[f]	1.681(4)
Angle		Cp1[a]–Cp[b]	3.5(3)
3			
Distances		C(1)–C(11)	1.446(8)
Fe(1)–C(Cp1[a])	2.045(6)–2.076(5)	Fe(2)–C(Cp3[c])	2.039(7)–2.068(6)
(Avg.)	2.059	(Avg.)	2.051
Fe(1)–C(Cp2[b])	2.041(7)–2.060(6)	Fe(2)–C(Cp4[d])	2.024(8)–2.037(9)
(Avg.)	2.052	(Avg.)	2.029
C–C(Cp1[a])	1.402(8)–1.426(8)	C–C(Cp3[c])	1.37(1)–1.43(1)
(Avg.)	1.418	(Avg.)	1.412
C–C(Cp2[b])	1.33(1)–1.42(1)	C–C(Cp4[d])	1.29(1)–1.43(1)
(Avg.)	1.381	(Avg.)	1.350
Fe(1)–Cp1[f]	1.669(3)	Fe(2)–Cp3[f]	1.662(4)
Fe(1)–Cp2[f]	1.682(4)	Fe(2)–Cp4[f]	1.671(7)
Angles		Cp1[a]–Cp3[c]	2.0(3)
Cp1[a]–Cp2[b]	2.2(3)	Cp3[c]–Cp4[d]	0.5(5)
4			
Distances		C(1)–C(11)	1.435(6)
Fe(1)–C(Cp1[a])	2.047(5)–2.129(4)	Fe(2)–C(Cp3[c])	2.030(5)–2.065(4)
(Avg.)	2.070	(Avg.)	2.045
Fe(1)–C(Cp2[b])	2.044(5)–2.125(4)	Fe(2)–C(Cp4[d])	2.029(6)–2.091(5)
(Avg.)	2.076	(Avg.)	2.050
C–C(Cp1[a])	1.406(8)–1.430(6)	C–C(Cp3[c])	1.382(9)–1.434(7)
(Avg.)	1.418	(Avg.)	1.414
C–C(Cp2[b])	1.400(8)–1.421(7)	C–C(Cp4[d])	1.40(1)–1.423(8)
(Avg.)	1.412	(Avg.)	1.409
Fe(1)–Cp1[f]	1.681(3)	Fe(2)–Cp3[f]	1.652(3)
Fe(1)–Cp2[f]	1.693(3)	Fe(2)–Cp4[f]	1.661(5)
Angles		Cp1[a]–Cp3[c]	0.7(3)
Cp1[a]–Cp2[b]	5.7(2)	Cp3[c]–Cp4[d]	5.3(4)

a) Cp1: C(1)–C(2)–C(3)–C(4)–C(5). b) Cp2: C(6)–C(7)–C(8)–C(9)–C(10). c) Cp3: C(11)–C(12)–C(13)–C(14)–C(15). d) Cp4: C(16)–C(17)–C(18)–C(19)–C(20). e) $-x+1, -y-1, -z+2$. f) Centroid.

tion, and the ferrocenyl ring of the adjacent donor is located above the alkyl chain, forming a stacked structure. The intermolecular Cp···Cp centroid distances between neighboring donors in compounds **1** and **2** are 5.50 and 5.41 Å, respectively. The Cp rings in the ferrocenium units exhibit eclipsed conformations, with the staggering angles being 5.1° for compound **1** and 5.9° for compound **2**. The intramolecular Fe–Fe distances are 5.147 and 5.134 Å for compounds **1** and **2**, respectively.

In these complexes, there are one-and-a-half crystallographically independent TCNQ molecules. In Figs. 3 and 4, the molecule denoted as A is located about crystallographic center of symmetry, although the intramolecular geometries of molecules A and B are the same within experimental error. Thus, the acceptor column is composed of a ...BAB BAB BAB...

Table 3. Bond Lengths (Å) for Acceptor Molecules in **1**–**4**

	1	**2**	**3**	**4**
a	1.348(6)–1.357(5)	1.345(5)–1.357(5)	1.356(7), 1.359(7)	1.351(6), 1.358(6)
(Avg.)	1.350	1.352	1.358	1.355
b	1.433(6)–1.438(6)	1.431(5)–1.441(5)	1.405(6)-1.416(6)	1.413(6)-1.421(6)
(Avg.)	1.435	1.436	1.410	1.418
c	1.385(6)–1.396(6)	1.383(5)–1.408(5)	1.408(7), 1.415(7)	1.409(6), 1.407(6)
(Avg.)	1.393	1.391	1.412	1.408
d	1.425(7)–1.436(7)	1.420(5)–1.433(5)	1.414(8)–1.433(7)	1.414(6)–1.428(6)
(Avg.)	1.430	1.429	1.426	1.421
e	1.138(6)–1.141(6)	1.133(6)–1.151(6)	1.139(7)–1.146(7)	1.133(6)–1.152(6)
(Avg.)	1.140	1.137	1.142	1.142
f	—	—	1.343(5)–1.349(5)	1.336(5)–1.347(5)
(Avg.)			1.347	1.343

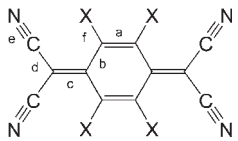

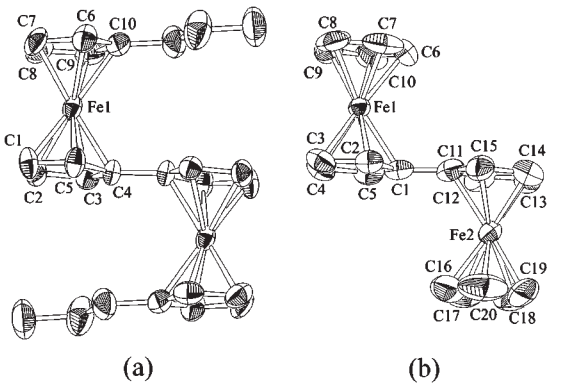

Fig. 2. ORTEP drawing of the cations in (1′,1‴-dipropyl-1,1′-biferrocenium)$^{+}$(TCNQ)$_3^{-}$ **1** and (biferrocenium)$^{+}$(F$_4$TCNQ)$^{-}$ **3** with the atom numbering scheme. Displacement ellipsoids are shown at the 50% probability level. Hydrogen atoms are omitted for clarity. The numbering scheme for the cations in **2** and **4** are the same as those for **1** and **3**, respectively.

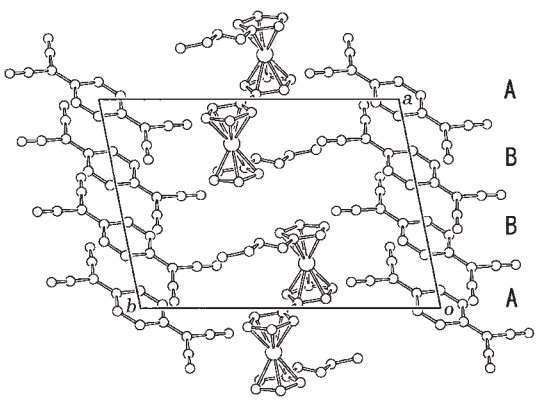

Fig. 4. Packing diagram of (1′,1‴-dibutyl-1,1′-biferrocenium)$^{+}$(TCNQ)$_3^{-}$ **2** viewed along the *a*-axis.

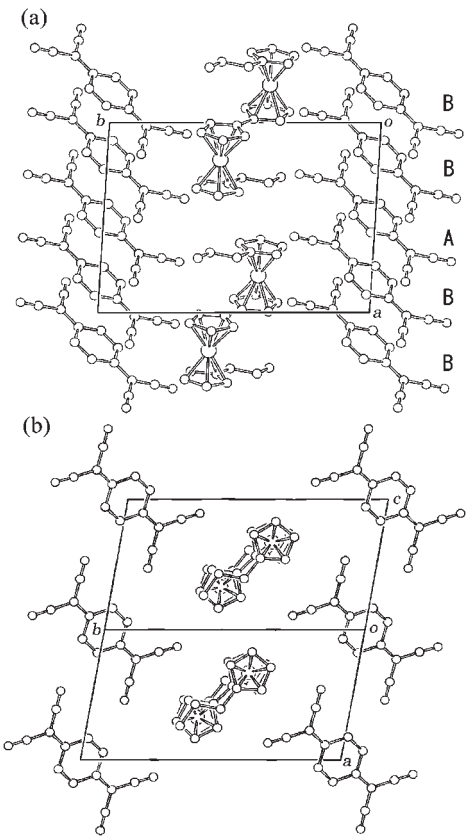

Fig. 3. Packing diagram of (1′,1‴-dipropyl-1,1′-biferrocenium)$^{+}$(TCNQ)$_3^{-}$ **1**. (a) Projection along the *a*-axis. (b) Projection along the stacking direction ($a + c$).

type of molecular stacking, exhibiting slight trimerization. The intratrimer and intertrimer distances between the TCNQ centroids in compound **1** are 3.76 and 3.80 Å, respectively, with the corresponding distances in compound **2** being 3.86 and 3.90 Å, respectively. Therefore, the degree of trimerization

is very slight in both complexes. The overlap integrals between the acceptors were calculated using the Hückel MO approximation to estimate qualitatively the degree of trimerization. The intratrimer and intertrimer overlap integrals in compound **1** were calculated to be 0.0149 and 0.0179, respectively, which indicates that the intertrimer interaction is slightly stronger than the intratrimer interaction. On the other hand, the corresponding overlap integrals for compound **2** were 0.0146 and 0.0144, which are virtually the same.

Crystal Structures of the Trapped-Valence Complexes. Structural determination of compounds **3** and **4** revealed that they have very different packing arrangements, despite having the same 1:1 D:A stoichiometry. Compound **3** exhibits a segregated-stack structure, while compound **4** exhibits a 2:2 mixed-stack structure. These compounds involve mixed-valence monocations.[20] Being consistent with this, the molecular geometries of the acceptors (Table 3) correspond to those of the F_4TCNQ monoanion.[28]

An ORTEP drawing of the molecular structure of the cations in compound **3** is shown in Fig. 2(b), and the packing diagram is shown in Fig. 5. Each component stacks along the *a*-axis. In the cation stacks, the Cp rings of the adjacent cations are located almost on the same plane. The Cp rings in the ferrocene units have near-eclipsed configurations, with staggering angles of 7.1 and 15°, for units Fc(1) and Fc(2), respectively. The intramolecular distance between the Fe(1) and Fe(2) sites is 5.073 Å. The average Fe–C(Cp) bond lengths are 2.056 Å for Fe(1) and 2.040 Å for Fe(2), which suggests that Fc(1) is closer to a ferrocenium state, and Fc(2) to a neutral state. Typical Fe–C(Cp) bond lengths for a ferrocenium state and a neutral state are 2.07 Å and 2.04 Å, respectively.[29,30] The Fe–C(Cp) distances are generally used as measures for the valence states of ferrocenes, although there is often a dispersion of the individual bond lengths. In the present compound, the Fe–Cp(centroid) distances, which are also used to estimate the valence state of ferrocenes, are consistent with the tendency found from the Fe–C distances. The former units, marked by dashed circles in Fig. 5, are located between neighboring F_4TCNQ anions with relatively short intermolecular Fe···NC– distances, whereas the latter units have no interactions with the acceptors.

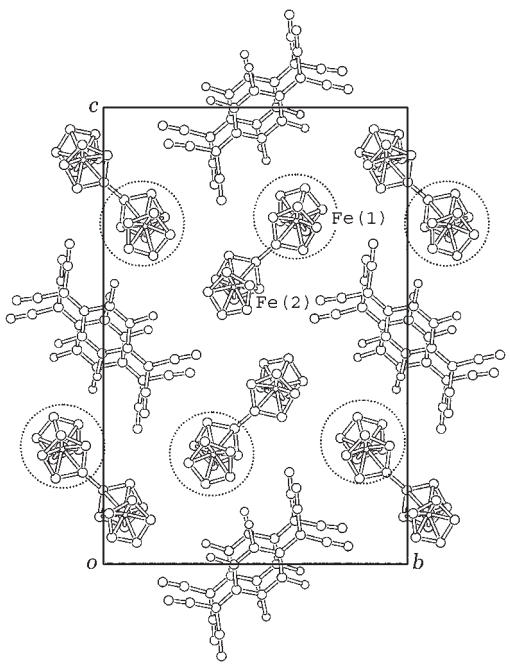

Fig. 5. Packing diagram of (biferrocenium)$^+$(F_4TCNQ)$^-$ **3**, projected along the *a*-axis. Dashed circles represent the ferrocenium units.

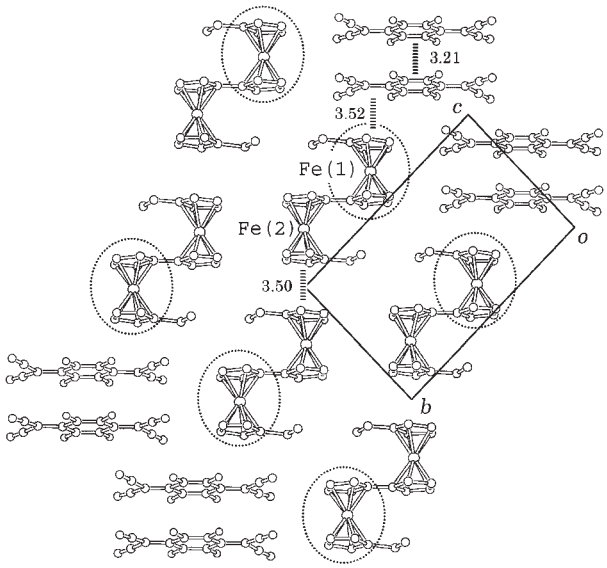

Fig. 6. Packing diagram of (1′,1‴-diethyl-1,1′-biferrocenium)$^+$(F_4TCNQ)$^-$ **4** viewed along the *a*-axis. Dashed circles represent the ferrocenium units. The dashed lines are merely guides to the eye.

The packing diagram of compound **4** is shown in Fig. 6. Dimers of the acceptor molecules and the donor molecules are stacked in an alternate fashion,

$$\ldots D^+D^+A^-A^-D^+D^+A^-A^- \ldots,$$

along the $a + 2b - 2c$ crystal direction, and the stacking structure forms a layer on the (2, −1, 0) plane. In the donor molecule, the average Fe–C(Cp) distance in the Fc(1) unit is 2.073 Å, and the average Fe–C(Cp) distance in the Fc(2) unit is 2.047 Å. This indicates that the Fc(1) corresponds to a ferrocenium unit, and Fc(2) corresponds to a neutral ferrocenyl unit. As can be seen in Fig. 6, the ferrocenium moieties, marked by dashed circles, are facing the molecular planes of the F_4TCNQ anions, and the neutral ferrocene moieties are facing towards the donor molecules. The neighboring distance between the Cp ring of the cation and the C=C bond of F_4TCNQ anion is 3.52 Å, and the intermolecular centroid distance between adjacent Cp rings within the donor dimer is 3.50 Å, as indicated in Fig. 6 by dashed lines. In addition, there are some other contact distances between the ferrocenium moieties and the neighboring acceptors, which are not shown in the figure, while the neutral ferrocene moieties have no contact with the acceptors. The intramolecular distance between the Fe(1) and Fe(2) units in the donor is 5.144 Å. The Cp rings have eclipsed conformations, with the staggering angles being 5.7 and 0° for Fc(1) and Fc(2), respectively.

In both complexes, the acceptor molecules are dimerized. In complex **3**, the distance between the centroids of the acceptor molecules within the dimer is 3.21 Å and the interdimer dis-

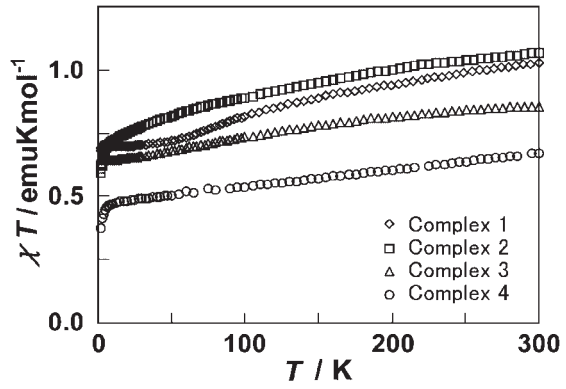

Fig. 7. Temperature dependence of the magnetic susceptibilities of **1**–**4** represented in the form of $\chi_m T$ vs T.

tance is 4.16 Å. In complex **4**, the centroid distance between the acceptor molecules within the dimer is 3.26 Å, and there is no interdimer contact. To estimate the degree of dimerization, we calculated the overlap integrals between the acceptor molecules. The intradimer and interdimer overlap integrals in compound **3** were calculated to be 0.0267 and 0.00287, respectively, which indicates that the degree of dimerization is strong, while the interdimer interaction is weak. In complex **4**, the intra-trimer overlap integral was 0.0252. These values are much larger than the overlap integrals between the non-dimerized acceptors in **1** and **2**.

Magnetic Susceptibility. Figure 7 shows the magnetic susceptibilities of compounds **1**–**4**, represented in the form of a χT versus T plot. In all the complexes, the contribution from the donor spins presumably dominates the magnetic susceptibility, because the acceptors in **1** and **2** are semiconducting and those in **3** and **4** are strongly dimerized. Indeed, similar magnetic behaviors have been observed in ferrocenium-related salts[31–33] and other biferrocenium salts with inorganic anions.[34,35] The χT values for ferrocenium ions at room temperature are usually ca. 0.7–0.9 emu K mol^{-1}, which are larger than the spin-only value because of the orbital contribution. The variation of the χT values of **1**–**4** may be ascribed to the alignment effect, owing to the anisotropy of the g-factor values.[36] The decrease of χT with decreasing temperature can be justified with a splitting of the ground $^2T_{2g}$ state by low symmetry components of the crystal field and spin–orbit coupling effects.[31,37] The magnetic data have been analyzed by using a modified Curie–Weiss expression, $\chi = C/(T+\theta) + q$, where q is temperature independent paramagnetism (TIP).[32,33] The parameters of best fit using the data below 100 K are shown in Table 4, and the result indicates the presence of only negligible magnetic interactions (<1 K). For compounds **3** and **4**, which contain dimerized acceptors, the data were also analyzed by applying a Curie–Weiss model for the donors and a dimer model (singlet–triplet model) to the acceptors, although the degree of fit was not satisfactory enough; the obtained parameters are $g_A = 2.0$ (Fix), $g_D = 2.69$, $\theta = -0.2$ K, $2J_{AA} = -365$ K for **3**, and $g_A = 2.0$ (Fix), $g_D = 2.35$, $\theta < -0.9$ K, $2J_{AA} = -537$ K for **4**. These results suggest the presence of very strong antiferromagnetic interactions between the acceptors. However, it should be noted that these analyses contain some ambiguity. We may at least conclude that these complexes are paramagnets with dominant contribution from the donor spins, although the larger susceptibility of compounds **1** and **2** than those of **3** and **4** may be ascribed to a larger contribution of the acceptors.

Table 4. Fitting Parameters of Magnetic Data for **1**–**4** (See Text)[a)]

Compound	C/emu K mol^{-1}	θ/K	$q/10^{-3}$ emu mol^{-1}
1	0.67	0.10	1.21
2	0.74	−0.48	1.63
3	0.63	0.07	1.07
4	0.49	−0.54	0.51

a) C: Curie constant, θ: Weiss constant, q: Temperature independent paramagnetism (TIP).

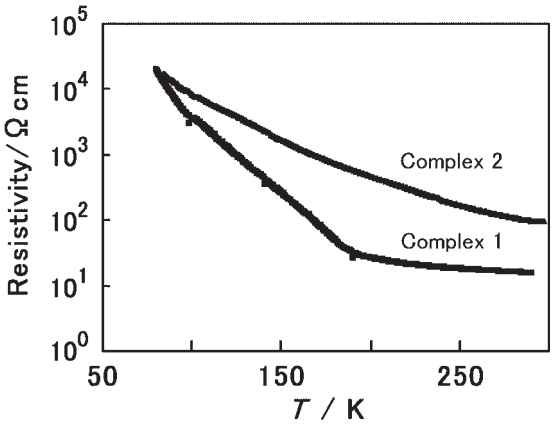

Fig. 8. Temperature dependence of the electrical resistivities of (1′,1‴-dipropyl-1,1′-biferrocenium)$^+$(TCNQ)$_3^-$ **1** and (1′,1‴-dibutyl-1,1′-biferrocenium)$^+$(TCNQ)$_3^-$ **2**.

Electrical Conductivity. The electrical conductivities of compounds **1** and **2** were measured to investigate the electron conduction along the TCNQ columns revealed by the structural analysis. Figure 8 shows the temperature dependence of the electrical resistivity of compounds **1** and **2**. Both compounds were semiconductors, with $\sigma_{RT} = 7 \times 10^{-2}$ S cm^{-1} and 5×10^{-2} S cm^{-1}, for compounds **1** and **2**, respectively. The resistivity of compound **1** shows an inflection point at around $T \sim 180$ K; the activation energy above this temperature is $E_a = 0.07$ eV (for $T = 190$–290 K) and below this temperature is 0.12 eV (for $T = 80$–140 K). The behavior was reversible with temperature change, and may possibly be associated with a structural change, but no anomaly was observed in a DSC measurement in the temperature range 90–330 K. The activation energy for compound **2** was $E_a = 0.06$ eV (for $T = 130$–290 K). Although metallic conductivity can be expected for a 1/6-filled TCNQ conduction band, these materials were semiconductors. Presumably, this can be ascribed to the one-dimensionality of the electronic structure, and to the narrow bandwidth derived from the small overlap integrals. Compounds **3** and **4** were insulators, which is consistent with the non-mixed-valency of the acceptors. Iijima et al. have pointed out the possibility of electrical conduction through TCNQ in (1′,1‴-diethyl-1,1″-biferrocenium)(TCNQ)$_2$,[38] which exhibits a high electrical conductivity in compacted pellets of $\sigma_{RT} = 1.5$ S cm^{-1}, and has $E_a = 0.064$ eV. In the present study, the stacked TCNQ structure has proven to be the rational conduction path.

Discussion

Origin of Contrasting Valence States in TCNQ and F_4TCNQ Salts. In this study, it was revealed that the origin of the stable averaged-valence states in the TCNQ complexes **1** and **2** is attributable to the symmetrical crystal environment around the cation and to the presence of the TCNQ columns. The dipole–dipole interactions between the cations are efficiently shielded by the columns, which have very large dielectric constants because of electrical conduction. On the other hand, the valence trapped states of the F_4TCNQ complexes **3** and **4** are found to be stabilized by electrostatic interactions between the anions and the cations and by the low crystal symmetry. Valence trapping due to electrostatic interactions is also found in biferrocenium tetrabromoferrate(1−),[30] in which the cation moiety is located closer to the anion. It is noted that the electrostatic interaction between the cations and anions in compound **3** is marginal because of the segregated structure, while the interaction is much stronger in compound **4** due to the direct π–π interactions. This structural difference reasonably accounts for the higher detrapping temperature of compound **4** observed by Mössbauer spectroscopy; The valence state of compound **3** becomes averaged when the temperature is elevated to $T = 320$ K, while that of compound **4** remains trapped.[20]

Effects of the Acceptors on the Resulting Valence States and Physical Properties. The TCNQ acceptors are much larger than inorganic anions, and they more easily interact with donors because of their planarity. The present study has demonstrated that these acceptors can shield the dipole–dipole interactions between the donors, as in compounds **1** and **2**, and can have strong face-to-face interactions with donors, as observed in compound **4**. Therefore, the donor–acceptor arrangements as well as cation–anion interactions were found to affect the valence states in these TCNQ complexes more severely than do those in inorganic salts. For biferrocenium salts containing inorganic anions, a linear correlation between the Cp tilt angle and the order–disorder valence transition temperature has been found by Dong et al.[39] They found that the rate of electron transfer increased as the tilt angle increased, which resulted in a lowering of the ordering temperature. In the present complexes, the Cp tilt angles are: 4.9° for compound **1**, 3.5° for compound **2**, 2.2° and 0.5° for compound **3**, and 5.7° and 5.3° for compound **4** (see Table 2). According to Dong's plot, the valence transition temperatures for these complexes are expected to fall between 250 and 330 K. The observed discrepancy demonstrates that electron transfer in organic charge-transfer complexes is highly influenced by the acceptors, and that the intramolecular geometry of the cation is less important.

In complexes **3** and **4**, the F_4TCNQ anions are dimerized. In the case of the ferrocene–TCNQ type complexes investigated by Miller et al., complexes with dimerized acceptors merely exhibit paramagnetism dominated by the contribution from the ferrocenium cations.[40] Therefore, using acceptors other than F_4TCNQ may be a more promising approach to realize intriguing magnetic properties, because F_4TCNQ anions often afford diamagnetic dimers. On the other hand, the acceptors are not dimerized in the TCNQ complexes of compounds **1** and **2**, although they showed no interesting magnetic properties because of the segregated-stack structures. In ferrocene–TCNQ type complexes, only the mixed-stack compounds with the …D–A–D–A… arrangement showed ferromagnetic interactions.[41] Therefore, future synthesis of biferrocenium salts with …D–A–D–A…-type mixed-stack arrangements may be interesting in terms of both magnetism and dielectric properties. The preparation of new biferrocene-based charge-transfer complexes using substituted TCNQ derivatives is in progress in our laboratories.

Conclusions

We have investigated the relationship between charge ordering, crystal structure, and electronic states in biferrocenium charge-transfer complexes with organic acceptors. The structure and properties of (1′,1‴-dipropyl-1,1′-biferrocenium)$^+$(TCNQ)$_3^-$, (1′,1‴-dibutyl-1,1′-biferrocenium)$^+$(TCNQ)$_3^-$, (biferrocenium)$^+$(F_4TCNQ)$^-$, and (1′,1‴-diethyl-1,1′-biferrocenium)$^+$(F_4TCNQ)$^-$ have been examined. The origin of the stable averaged-valence states in the former two complexes is attributable to the symmetrical crystal environment around the cation and to the presence of the TCNQ columns, while that for charge localization in the latter two is ascribable to the electrostatic interactions between the cations and the anions. The influence of the acceptors on the valence states is considered to be much more pronounced than that of inorganic counter anions. These findings may be helpful for designing charge-transfer materials with functions based on electron-transfer.

This work was financially supported by PRESTO, JST (Japan Science and Technology Corporation). We thank Mr. Kousuke Takazawa (Toho University) for data analysis and Ms. Eri Nagabuchi for DSC measurements. We also thank Mr. Masaru Nakama (WarpStream Ltd., Tokyo) for constructing Web-DB systems.

References

1 D. N. Hendrickson, "Mixed Valency Systems: Applications in Chemistry, Physics, and Biology," ed by K. Prassides, Kluwer, Dordrecht (1991).

2 "Mixed-Valence Compounds: Theory and Applications in Chemistry, Physics, Geology, and Biology," ed by D. B. Brown, Reidel, Dordrecht (1980).

3 P. Day, *Int. Rev. Phys. Chem.*, **1**, 149 (1981).

4 C. Creutz, *Prog. Inorg. Chem.*, **30**, 1 (1983).

5 D. E. Richardson and H. Taube, *Coord. Chem. Rev.*, **60**, 107 (1984).

6 H. Sano, *Hyperfine Interact.*, **53**, 97 (1990).

7 S. Nakashima, Y. Ueki, H. Sakai, and Y. Maeda, *J. Chem. Soc., Dalton Trans.*, **1996**, 139.

8 S. Nakashima, *Recent Res. Dev. Pure Appl. Chem.*, **2**, 247 (1998).

9 S. Nakashima, T. Oda, T. Okuda, and M. Watanabe, *Inorg. Chem.*, **38**, 4005 (1999).

10 T.-Y. Dong, L.-S. Chang, G.-H. Lee, and S.-M. Peng, *Organometallics*, **21**, 4192 (2002).

11 T.-Y. Dong, P.-H. Ho, X.-Q. Lai, Z.-W. Lin, and K.-J. Lin, *Organometallics*, **19**, 1096 (2000).

12 R. J. Webb, T. Y. Dong, C. G. Pierpont, S. R. Boone, R. K. Chadha, and D. N. Hendrickson, *J. Am. Chem. Soc.*, **113**, 4806

(1991).
13 D. N. Hendrickson, S. M. Oh, T.-Y. Dong, T. Kambara, M. J. Cohn, and M. F. Moore, *Comments Inorg. Chem.*, **4**, 329 (1985).
14 J. S. Miller, A. J. Epstein, and W. M. Reiff, *Angew. Chem., Int. Ed. Engl.*, **33**, 385 (1994).
15 T. Mochida, *Mol. Cryst. Liq. Cryst.*, **343**, 205 (2000).
16 T. Mochida, S. Suzuki, and H. Moriyama, *Mol. Cryst. Liq. Cryst.*, **376**, 477 (2002).
17 T. Mochida, H. Matsui, S. Suzuki, and H. Moriyama, *Mol. Cryst. Liq. Cryst.*, **376**, 295 (2002).
18 S. Nakashima, S. Iijima, I. Motoyama, M. Katada, and H. Sano, *Hyperfine Interact.*, **40**, 315 (1988).
19 S. Iijima, R. Saida, I. Motoyama, and H. Sano, *Bull. Chem. Soc. Jpn.*, **54**, 1375 (1981).
20 S. Iijima and F. Mizutani, *Mol. Cryst. Liq. Cryst.*, **322**, 79 (1998).
21 T. Mochida, S. Yamazaki, E. Nagabuchi, S. Ebiwasa, and H. Mori, to be published.
22 T. Mori, A. Kobayashi, Y. Sasaki, H. Kobayashi, G. Saito, and H. Inokuchi, *Bull. Chem. Soc. Jpn.*, **57**, 627 (1984).
23 A. Altomare, G. Cascarano, C. Giacovazzo, A. Guagliardi, M. C. Burla, G. Polidori, and M. Camalli, *J. Appl. Crystallogr.*, **27**, 435 (1994).
24 "teXsan: Crystal Structure Analysis Package," Molecular Structure Corporation, The Woodlands, Texsas (1999).
25 "CrystalStructure, Single Crystal Structure Analysis Software. Version 3.1.," Molecular Structure Corporation, The Woodlands, TX, USA, and Rigaku Corporation, Akishima, Tokyo, Japan (2002).
26 J. S. Miller, J. H. Zhang, W. M. Reiff, D. A. Dixon, L. D. Preston, A. H. Reis, Jr., E. Gebert, M. Extine, J. Troup, A. J. Epstein, and M. D. Ward, *J. Phys. Chem.*, **91**, 4344 (1987).
27 "ORTEP-3 for Windows;" L. J. Farrugia, *J. Appl. Crystallogr.*, **30**, 565 (1997).
28 J. S. Miller, J. H. Zhang, and W. M. Reiff, *Inorg. Chem.*, **26**, 600 (1987).
29 A. C. Macdonald and J. Trotter, *Acta Crystallogr.*, **17**, 872 (1964).
30 S. J. Geib, A. L. Rheingold, T.-Y. Dong, and D. N. Hendrickson, *J. Organomet. Chem.*, **312**, 241 (1986).
31 D. N. Hendrickson, Y. S. Shon, and H. B. Gray, *Inorg. Chem.*, **10**, 1559 (1971).
32 S. Zürcher, J. Petrig, M. Perseghini, V. Gramlich, M. Wörle, and A. Togni, *Helv. Chim. Acta*, **82**, 1324 (1999).
33 S. Zürcher, J. Petrig, V. Gramlich, M. Wörle, C. Mensing, D. v. Arx, and A. Togni, *Organometallics*, **18**, 3679 (1999).
34 W. H. Morrison, Jr., S. Krogsrud, and D. N. Hendrickson, *Inorg. Chem.*, **12**, 1998 (1973).
35 D. O. Cowan, G. A. Candela, and F. Kaufman, *J. Am. Chem. Soc.*, **93**, 3889 (1971).
36 J. S. Miller, D. T. Glatzhofer, C. Vazquez, R. S. McLean, J. C. Calabrese, W. J. Marshall, and J. W. Raebiger, *Inorg. Chem.*, **40**, 2058 (2001).
37 B. N. Figgis, M. Gerloch, and R. Mason, *Proc. R. Soc. London, Ser. A*, **309**, 91 (1969).
38 S. Iijima and Y. Tanaka, *J. Organomet. Chem.*, **270**, C11 (1984).
39 T.-Y. Dong, H.-H. Lee, C.-K. Chang, H.-M. Lin, and K.-J. Lin, *Organometallics*, **16**, 2773 (1997).
40 J. S. Miller, J. H. Zhang, W. M. Reiff, D. A. Dixon, L. D. Preston, A. H. Reis, E. Gebert, M. Extine, J. Troup, A. J. Epstein, and M. D. Ward, *J. Phys. Chem.*, **91**, 4344 (1987).
41 J. S. Miller, A. J. Epstein, and W. M. Reiff, *Chem. Rev.*, **88**, 201 (1988).